Journal of Applied Mathematics and Physics, 2017, 5, 1908-1916
http://www.scirp.org/journal/jamp
ISSN Online: 2327-4379
ISSN Print: 2327-4352

Bifurcations and Chaos in the Duffing Equation with One Degenerate Saddle Point and Single External Forcing

Zhiyang Yang, Tao Jiang

School of Information, Beijing Wuzi University, Beijing, China
Email: zyyang@amss.ac.cn, taojiang@amss.ac.cn

How to cite this paper: Yang, Z.Y. and Jiang, T. (2017) Bifurcations and Chaos in the Duffing Equation with One Degenerate Saddle Point and Single External Forcing. *Journal of Applied Mathematics and Physics*, **5**, 1908-1916.
https://doi.org/10.4236/jamp.2017.59161

Received: August 4, 2017
Accepted: October 13, 2017
Published: October 16, 2017

Abstract

In this paper, we study the Duffing equation with one degenerate saddle point and one external forcing and obtain the criteria of chaos of Duffing equation under periodic perturbation through Melnikov method. Numerical simulations not only show the correctness of the theoretical analysis but also exhibit the more new complex dynamical behaviors, including homoclinic bifurcation, bifurcation diagrams, maximum Lyapunov exponents diagrams, phase portraits and Poincaré maps.

Keywords

Duffing Equation, Melnikov Method, Numerical Simulations

1. Introduction

Since in 1918, the German electrical engineer Georg Duffing introduced the Duffing equation, many scientists have been widely studied the equation in physics, economics, engineering, and found many other physical phenomena. The Duffing oscillator, is normally written as

$$\ddot{x}+\delta\dot{x}+\beta x+\alpha x^3 = F\cos(\omega t). \tag{1}$$

Depending on the parameters chosen, the equation can take a number of special forms. For example, Bender and Orszag [1] and Zwillinger [2] took the parameters $\delta=0, F=0$ and studied the Duffing Equation (1) with no damping and no forcing,

$$\ddot{x}+\beta x+\alpha x^3 = 0. \tag{2}$$

Wiggins [3] took $\beta=-1, \alpha=1$ and studied the following Duffing equation

$$\ddot{x}+\delta\dot{x}-x+x^3=F\cos(\omega t). \tag{3}$$

Ravichandran *et al.* [4] replaced the external forcing $F\cos(\omega t)$ as various periodic external forcing. Equation (3) with one external forcing and two potential wells has many different types of oscillations such as chaos and limit cycles [5]. And Huang and Jing [6] studied the three well Duffing equation with one external forcing

$$\begin{aligned}\dot{x}&=y,\\ \dot{y}&=-x(x^2-1)(x^2-a)-\delta y+f\cos(\omega t),\end{aligned} \tag{4}$$

and obtained the conditions of existence and bifurcations for harmonics, subharmonics and superharmonics under small perturbations and the threshold values of chaotic motion under periodic perturbation. And Jing *et al.* [7] [8] obtained complex dynamics of the three well Duffing equation with two external forcings,

$$\begin{aligned}\dot{x}&=y,\\ \dot{y}&=-x(x^2-1)(x^2-a)+\delta y+f_1\cos(\omega_1 t)+f_2\cos(\omega_2 t).\end{aligned} \tag{5}$$

Wang [9] presented analytical and numerical results concerning the inhibition of chaos in the Duffing equation with two weak forcing excitations. Jiang *et al.* [10], studied bifurcation and chaos of the three well Duffing equation with parametric excitation and one external forcing

$$\begin{aligned}\dot{x}&=y,\\ \dot{y}&=-x(x^2-1)(x^2-a^2)+f\cos(\omega t)+bx\cos(\Omega t).\end{aligned} \tag{6}$$

But less attention was focused on the two well Duffing equation with one degenerated saddle. In this paper we studied the following Duffing equation

$$\begin{aligned}\dot{x}&=x,\\ \dot{y}&=-x^3(x^2-1)-\delta y+f\cos(\omega t),\end{aligned} \tag{7}$$

where δ, f, ω are real parameters. Physically, δ can be regarded as dissipation or damping; f and ω is the amplitude and frequency of the external force.

The structure of the paper is as follows. In Section 2, the fixed points and phase portraits are obtained for the unperturbed system of (7). In Section 3, the conditions of existence of chaos under periodic perturbation resulting from the homoclinic bifurcations are performed by Melnikov method. Finally, we make some numerical computations which give support to the theoretical analysis and some complex dynamics in Section 4.

2. Fixed Points and Phase Portrait of Unperturbed System of (7)

In this section, we obtain the stability of fixed points and phase portrait of unperturbed system of (7).

For we take $\delta=f=0$ and obtain the unperturbed system of (7) as follows

$$\begin{aligned} \dot{x} &= y, \\ \dot{y} &= -x^3(x^2-1). \end{aligned} \tag{8}$$

The unperturbed system (7) can be easily obtained three fixed points: a degenerate saddle $S(0,0)$ and two centers $C_1(-1,0)$ and $C_2(1,0)$. The phase portrait of the unperturbed system (7) is plotted in **Figure 1**. The degenerate saddle is connected by two homoclinic orbits

$\Gamma_1(x_0(t), y_0(t)) = (-\frac{\sqrt{6}}{\sqrt{4+3t^2}}, \frac{3\sqrt{6}t}{\sqrt{(4+3t^2)^3}})$ and

$\Gamma_2(x_0(t), y_0(t)) = (\frac{\sqrt{6}}{\sqrt{4+3t^2}}, -\frac{3\sqrt{6}t}{\sqrt{(4+3t^2)^3}})$, respectively.

In essence we use perturbation methods to study the system (7), we therefore study how the dynamics of unperturbed system (8) are changed under the periodic perturbation in the following parts.

3. Chaos for Periodic Perturbations

In this section, we consider the chaotic behaviors of system (7) in which δ, f are assumed to be small parameters with order ε. The Duffing system can be written an as follows:

$$\begin{aligned} \dot{x} &= y, \\ \dot{y} &= -x^3(x^2-1) + \varepsilon(-\delta_1 y + f_1 \cos(\omega t)), \end{aligned} \tag{9}$$

where $\varepsilon\delta_1 = \delta, \varepsilon f_1 = f$.

The closed homoclinic orbits break when the perturbation is added, and system (7) may have transverse homoclinic orbits. By the Smale-Birkhoff Theorem [3] [11] [12], the existence of such orbits may results in chaotic dynamics. Therefore, we apply the Melnikov method to system (7) for finding the criteria of the existence of homoclinic bifurcation and chaos.

For the homoclinic orbit Γ_1, we have the Melnikov function,

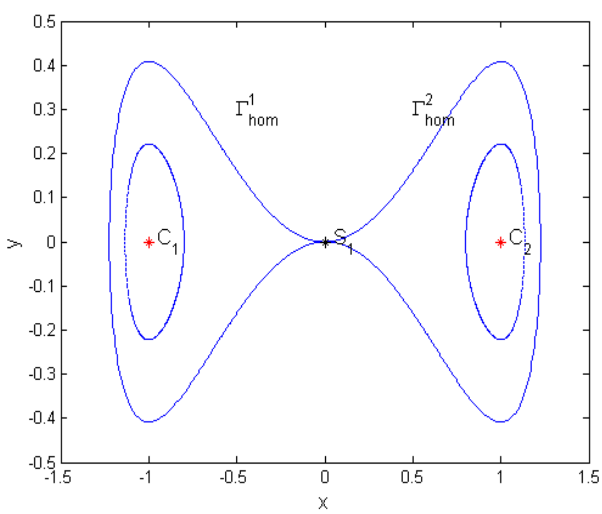

Figure 1. Phase portrait of system (8).

$$\begin{aligned} M_1(t_0; f_1, \delta_1, \omega) &= \int_{-\infty}^{+\infty} y_0(t)(-\delta_1 y_0(t) + f_1 \cos(\omega(t+t_0)))dt \\ &= -\frac{3}{32}\sqrt{3}\pi\delta_1 + 2\sqrt{2} f_1 \omega \sin(\omega t_0) BesselK(0, \frac{2\omega}{\sqrt{3}}), \end{aligned} \tag{10}$$

where $BesselK(0, \frac{2\omega}{\sqrt{3}})$ is Bessel functions of the second. If we define

$$R^0(\omega) = \frac{3\sqrt{3}\pi}{64\sqrt{2}\omega BesselK(0, \frac{2\omega}{\sqrt{3}})}, \tag{11}$$

then it follows from Theorem 4.5.3 in [11] that if $f_1 / \delta_1 > R^0(\omega)$, the stable manifold of the fixed point (0,0) intersects the unstable manifold for ε sufficiently small, and if $f_1 / \delta_1 < R^0(\omega)$, the stable manifold doesn't intersect the unstable manifold. Moreover, since $M_1(t_0; f_1, \delta_1, \omega)$ has quadratic zeros when $f_1 / \delta_1 = R^0(\omega)$, there is a bifurcation curve of system (9) in the $(f_1, -\delta_1)$ plane for each fixed ω, tangent to $f_1 = R^0(\omega)\delta_1$ at $f_1 = \delta_1 = 0$. This implies that if $\varepsilon > 0$ is sufficiently small, the transverse heteroclinic orbits exist and system (9) may be chaotic. In **Figure 2**, we give the diagram of (11) in $\omega - R^0(\omega)$ plane for $\omega \in [0, 2]$.

For the homoclinic orbit Γ_2, the computation is identical and the similar result is obtained.

4. Numerical Simulations

In this section we give numerical simulations to look for other new dynamics. In the process of numerical simulation, we vary one parameter and fix the other parameters of system (7) as follows:

1) Varying f in the range $0 \le f \le 5$ and fixing $\delta = 0.2$ and for rational and irrational values of ω.

2) Varying δ in the range $0 \le \delta \le 2$ and fixing $f = 1$ and for rational and irrational values of ω.

For case 1). The bifurcation diagram of system (7) in (f, x) plane and the corresponding Lyapunov exponents for $\delta = 0.2, \omega = 2$ are given in **Figure 3(a)** and **Figure 3(b)**, respectively. We observe that a period-1 window for $0 < f < 0.333$ becomes chaos at $f = 0.333$ and chaos at 1.391 becomes a period-1 window for $1.392 < f \le 5$. From **Figure 3(c)**, the local amplification of **Figure 3(a)** for $0.55 \le f \le 0.6$, there exist three period-doubling bifurcation to chaos for $0.5523 < f < 0.588$.

The bifurcation diagram of system (7) in (f, x) plane and the corresponding Lyapunov exponents for $\delta = 0.2, \omega = \sqrt{2}/2$ are given in **Figure 4(a)** and **Figure 4(b)**, respectively. A period-1 window suddenly becomes chaos at $f = 0.203$ and chaoticmotion suddenly becomes a period-doubling bifurcation at $f = 0.212$. And for $0.213 < f < 5$ period-doubling bifurcation to chaos and chaos to period-doubling bifurcations alternatively appear. Poincaré maps of chaotic attractors for $f = 0.21, f = 0.85$ and $f = 4.95$ are shown in **Figures 4(c)-(e)**, respectively.

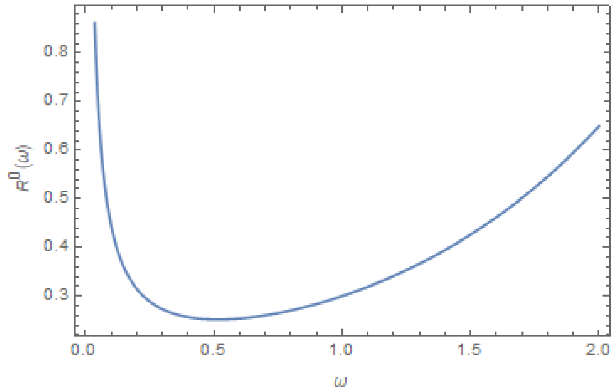

Figure 2. The diagram of (11) in $\omega - R^0(\omega)$ plane.

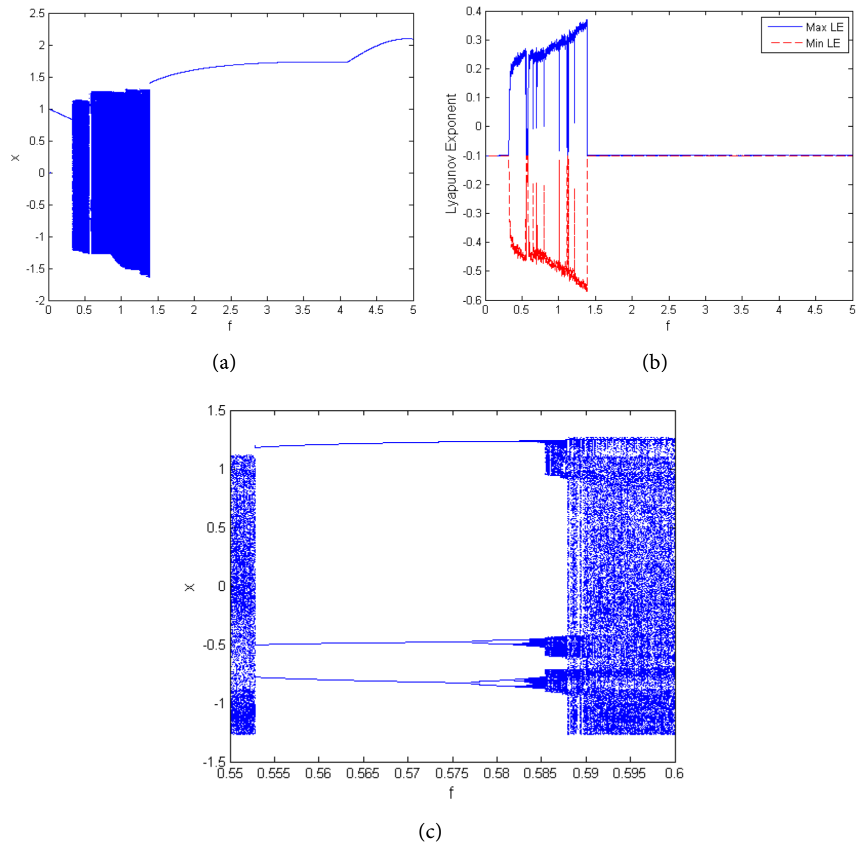

Figure 3. (a) Bifurcation diagram of system (7) for $\delta = 0.2, \omega = 2$; (b) Lyapunov exponents corresponding to (a); (c) Local amplification of (a) for $0.55 \le f \le 0.6$.

For case 2). The bifurcation diagram of system (7) in (f, x) plane and the corresponding Lyapunov exponents for $f = 1, \omega = 2$ are given in **Figure 5(a)** and (b). There exist onset of chaos at $\delta = 0.28$ from a period-1 window for $0 < \delta < 0.279$. And chaos suddenly becomes three inverse period-doubling bifurcation at $\delta = 0.246$. We observe that chaos to inverse period-doubling bifurcations and inverse period-doubling bifurcations to chaos alternatively appear. And the size of chaotic attractors becomes smaller at $\delta = 0.622$ that an

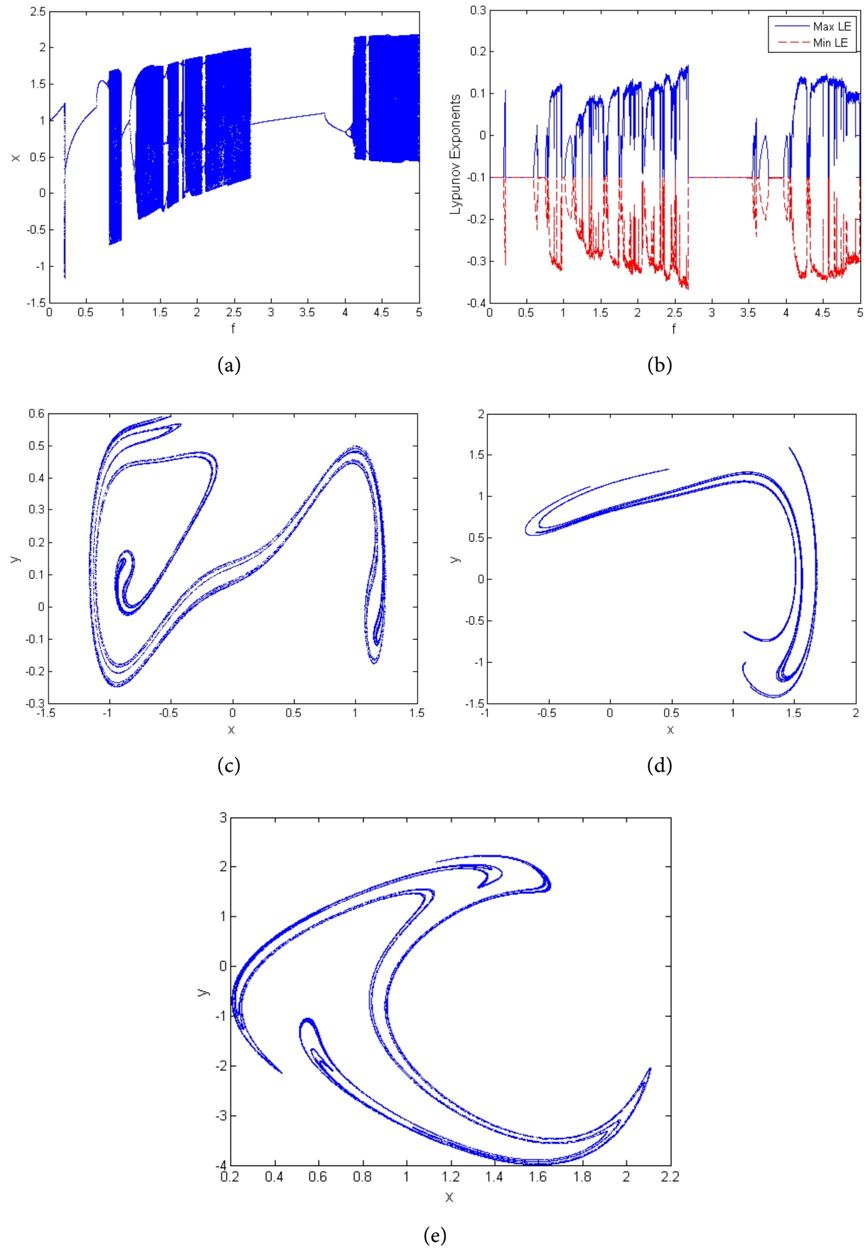

Figure 4. (a) Bifurcation diagram of system (7) for $\delta = 0.2, \omega = \sqrt{2}/2$. (b) Lyapunov exponents corresponding to (a). (c)-(e) Poincaré maps for $f = 0.21, f = 0.85$ and $f = 4.95$, respectively

interior crisis occurs. Poincaré maps of chaotic attractors for $\delta = 0.621$ and $\delta = 0.622$ are shown in **Figure 5(c)** and **Figure 5(d)**, respectively.

The bifurcation diagram of system (7) in (f, x) plane and the corresponding Lyapunov exponents for $f = 1, \omega = \sqrt{2}/2$ are given in **Figure 6(a)** and **Figure 6(b)**. Period-2 orbit becomes period-1 orbit at $\delta = 0.09$. From the local amplification **Figure 6(c)** of **Figure 6(a)**, a period-1 window disappears and chaos appear at $\delta = 0.276$. There exists an interior crisis of chaos at $\delta = 0.314$ and chaos regions becomes inverse period-doubling bifurcations to period-doubling

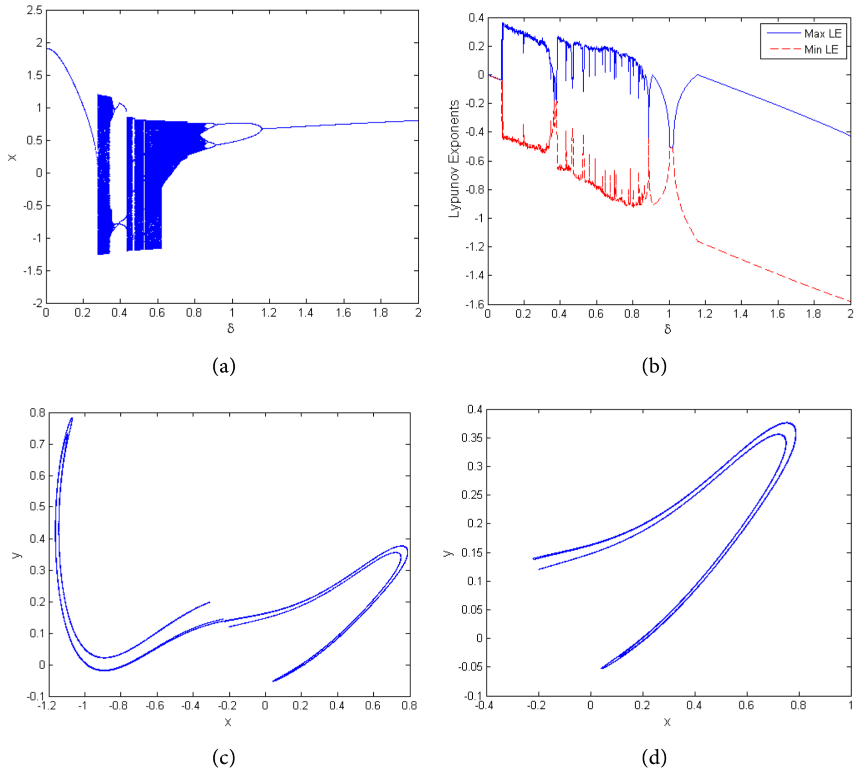

Figure 5. (a) Bifurcation diagram of system (7) for $f = 1, \omega = 2$. (b) Lyapunov exponents corresponding to (a). (c)-(d) Poincaré maps for $\delta = 0.621$ and $\delta = 0.622$, respectively.

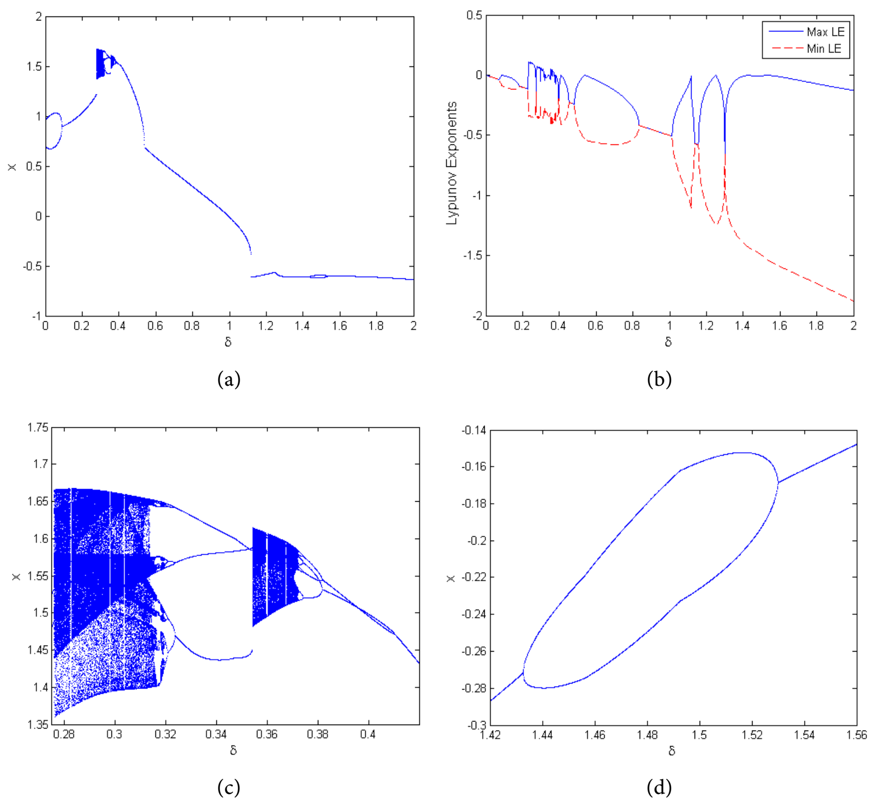

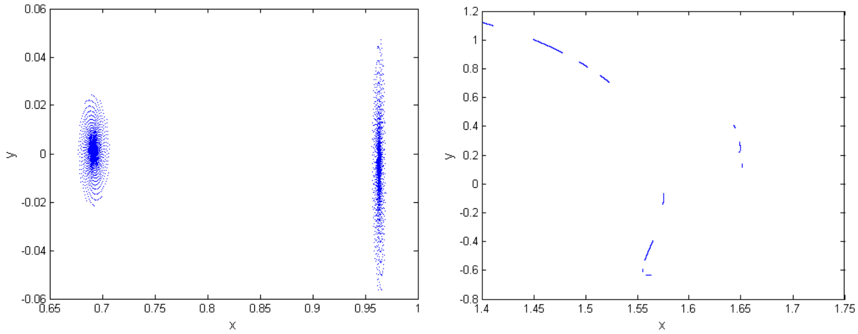

(e) (f)

Figure 6. (a) Bifurcation diagram of system (7) for $f=1, \omega=\sqrt{2}/2$. (b) Lyapunov exponents corresponding to (a). (c) and (d) Local amplification of (a) for $0.275 \le \delta \le 0.42$ and $1.42 < \delta < 1.56$, respectively. (e)-(f) Poincaré maps for $\delta = 0$ and $\delta = 0.316$, respectively.

bifurcations for $0.315 < \delta < 0.325$. At $\delta = 0.3541$ an intermittence of chaos occurs and chaotic motion becomes inverse period-doubling bifurcation. There is a bubble for $1.432 < \delta < 1.531$ in the local amplification **Figure 6(d)** of **Figure 6(a)**. Poincaré map for $\delta = 0$ is shown in **Figure 6(e)**. Poincaré map of chaotic attractor for $\delta = 0.316$ is shown in **Figure 6(f)**.

Acknowledgements

This work was supported by the National Science Foundations of China (10671063, 10801135 and 61571052).

References

[1] Bender, C.M. and Orszag, S.A. (1978) Advanced Mathematical Methods for Scientists and Engineers. McGraw-Hill, New York.

[2] Zwillinger, D. (1997) Handbook of Differential Equations. 3rd ed., Academic Press, New York.

[3] Wiggins, S. (1987) Chaos in the Quasi Periodically Forced Duffing Oscillator. *Physics Letters A*, **124**, 138-142.

[4] Ravichandran, V., Chinnathambi, V. and Rajaekar, S. (2006) Effect of Various Periodic Forces on Duffing Oscillator. *Pramana-Journal of Physics*, **67**, 351-356.

[5] Holmes, C. and Holmes, P. (1981) Second Order Averaging and Bifurcations to Subharmonics in Duffing's Equation. *Journal of Sound and Vibration*, **78**, 161-174.

[6] Huang, J.C. and Jing, Z.J. (2009) Bifurcations and Chaos in Three-Well Duffing System with One External Forcing. *Chaos, Solitons and Fractals*, **40**, 1449-1466.

[7] Jing, Z.J., Huang, J.C. and Deng, J. (2007) Complex Dynamics in Three-Well Duffing System with Two External Forcings. *Chaos, Solitons and Fractals*, **33**, 795-812.

[8] Jing, Z.J. and Wang, R.Q. (2005) Complex Dynamics in Duffing System with Two External Forcings. *Chaos, Solitons and Fractals*, **23**, 399-411.

[9] Wang, R.Q., Deng, J. and Jing, Z.J. (2006) Effect of Various Periodic Forces on Duffing Oscillator. *Chaos, Solitons and Fractals*, **27**, 249-257.

[10] Jiang, T., Yang, Z.Y. and Jing, Z.J. (2017) Bifurcations and Chaos in the Duffing

Equation with Parametric Excitation and Single External Forcing. *International Journal of Bifurcation and Chaos*, **27**, 1750125-1-31.

[11] Guckenheimer, J. and Holmes, P. (1993) Nonlinear Oscillation and Bifurcation of Vector Fields. Springer-Verlag, New York.

[12] Guckenheimer, J. and Holmes, P. (1997) Dynamical Systems and Bifurcations of Vector Fields. Springer-Verlag, New York.